ORNL/SPR-2022/2503

# *Initial Microstructure Examination of High Burnup Fuel with Varying Operational Burnups*

## Nuclear Technology Research and Development

**Approved for public release.**
**Distribution is unlimited.**

***Prepared for***
***US Department of Energy***
***Nuclear Technology R&D Program***
***Advanced Fuels Campaign***
***R.L. Seibert, J.W. Werden, C.M. Parish,***
***J.M. Harp, T.J. Gerczak, and N.A. Capps***
***Oak Ridge National Laboratory***
***June 17th 2022***
***M3FT-22OR020205023***

# SUMMARY

This report presents an initial examination of the microstructure of high burnup $UO_2$ under pre- and post-loss of coolant accident (LOCA) conditions. This work builds upon work previously conducted on high burnup $UO_2$ fuel at Oak Ridge National Laboratory. Studying microstructure evolutions that occur in $UO_2$ during irradiation, particularly in high burnup fuel, will provide a deeper understanding of fuel fragmentation under simulated LOCA conditions. High burnup $UO_2$ microstructural data is also needed to improve constitutive models intended to predict high burnup fuel fragmentation. The objective of this work is to begin the process of examining high burnup fuel microstructural features before and after LOCA testing to better understand mechanisms driving experimental observations. Several high burnup fuel samples were available from historic fuel shipments to ORNL. These samples were leveraged along with state-of-the-art microscopy capabilities. This report summarizes the current ongoing work using these fuel samples to interpret and analyze high burnup fuel microstructures.

This page is intentionally left blank.

# CONTENTS

This page is intentionally left blank.

# FIGURES

# ACRONYMS

| | |
|---|---|
| EBSD | electron backscatter diffraction |
| EDS | energy dispersive x-ray spectroscopy |
| FFRD | fuel fragmentation relocation and dispersal |
| FGR | fission gas release |
| FIB | focused ion beam |
| HAGB | high angle grain boundaries |
| HBFF | high burnup fuel fragmentation |
| HBS | high burnup structure |
| LAGB | low angle grain boundaries |
| LOCA | loss-of-coolant accident |
| SEM | scanning electron microscopy |
| S/TEM | scanning transmission electron microscopy |
| tFGR | transient fission gas release |

# INITIAL MICROSTRUCTURE EXAMINATION OF HIGH BURNUP FUEL WITH VARYING OPERATIONAL HISTORIES

## 1. INTRODUCTION

Fuel fragmentation relocation and dispersal (FFRD) is an engineering scale phenomenon observed in high burnup fuel under loss-of-coolant accident (LOCA) conditions. The phenomenon was first observed in the early to mid 2000s following high burnup LOCA experiments performed at the Halden Boiling Water test reactor. In these tests, high burnup fuel (>80 GWd/tU) suffered significant fragmentation and pulverization. This behavior has since been termed high burnup fuel fragmentation (HBFF), where fuel pellets fragment with an effective consistency of sand [1-3]. Subsequently, pulverized fuel could relocate into the cladding balloon region and, following cladding rupture, disperse from the cladding. The issue gained further attention when HBFF was observed closer to the current U.S. Nuclear Regulatory Commision (NRC) burnup limit (62 GWd/tU) during NRC-sponsored out-of-core integral tests at Studsvik Nuclear in early 2011 [4,5]. The experimental results identified a burnup range between 65–72 GWd/tU where the fuel pellet begins to pulverize and become susceptible to relocation and dispersion. The combination of HBFF, relocation and dispersal has since been termed FFRD. HBFF research to date has come to similar conclusions [1-11]. Engineering scale LOCA tests have determined that cladding behavior, pellet history, and LOCA test conditions impact the severity of HBFF, but engineering data have shed little light to the mechanism driving HBFF and subsequent consequences. The current working theory is that the mechanisms driving HBFF are related to lower length scale behaviors.

In parallel, sub-micron grains have been observed near the rim of high burnup fuel that may enhance fission gas release (FGR) during steady state operation. It is also hypothesized that due to the storage of fission gas in the rim region, large amounts of fission gas could be released during transient or off-normal heating conditions [12-21]. Separate effects test programs developed out-of-pile heating techniques with an emphasis on applying hydrostatic pressures under controlled conditions. The aim was to investigate the impact of an external hydrostatic pressure on FGR and swelling of fission gas bubbles. In summary, FGR strongly depended on the extent of rim structure formation and heating conditions (i.e., heating rate and terminal temperature). Experimental results indicated that the growth and interlinkage of intergranular bubbles in the rim structure controlled FGR above threshold temperatures (~1000 $^{o}$C), whereas burst release of fission gas from high heating rates originated from the formation of microcracks in the rim region. This microcracking ultimately resulted in extensive fuel fragmentation and eventual pulverization. Similar behavior increases in transient FGR (tFGR) were observed during pellet annealing tests as shown in Figure 1. Low burnup tFGR primarily occurred when fuel temperatures exceeded ~1000 $^{o}$C, whereas high burnup (>71 GWd/tU) fuel experienced a burst release of fission gas initiating at ~550 $^{o}$C and completing at ~800 $^{o}$C. Post-test evaluations of the high burnup fuel pellets indicated that microcracking was likely responsible for the observed burst release of fission gas. Microcracking is most often observed in susceptible microstructures that could include sub-micron grains and high fission gas concentrations that render the local material weaker and more susceptible to cracking.

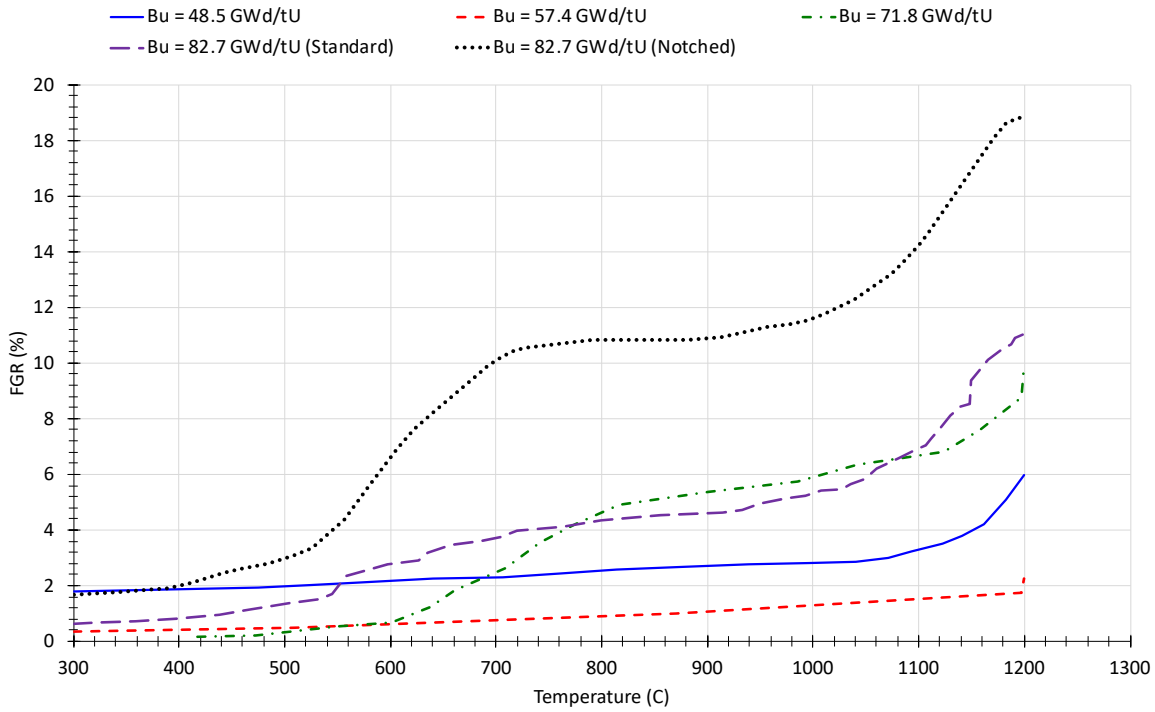


Figure 1. tFGR data from the GASPARD FGR program for various average pellet burnups [22-24]

It seems straight forward to suggest that the mechanism driving HBFF is attributed to rapid fission gas bubble expansion in the vicinity of fully re-structured sub-micron grains (e.g., weakened microstructure) in the rim region; however, the rim region only represents a small portion (<10%) of the total fuel volume and fails to capture the extent of HBFF observed in engineering scale LOCA tests. This would suggest that other mechanisms may drive HBFF in the pellet mid-radius region and/or that other microstructural features are rendering the fuel suspectable to HBFF in this region. Gerczak et. al. [25] used modern microscopy techniques to investigate restructuring in high burnup fuel. The microscopy survey indicated the onset of restructuring occurring in the mid-radial region of the pellet. This result does not explain why HBFF occurs in this region; however, it does indicate signs of pellet weakening in the mid-radius region that may contribute to the mechanism driving HBFF in the mid-pellet region.

In an effort to better understand the mechanisms driving HBFF and how the microstructural characteristics impact the fuel performance, advanced microscopy techniques will be used to assess high burnup fuel prior to and following a simulated LOCA. The intent is to replicate the work done by Gerczak et. Al. [25]. A lengthy background on the current understanding of HBS is discussed in [25,26] and is briefly summarized here: HBS formation is proposed to start either from nucleation and growth, or from polygonization, which is the subdivision of grains due to the arrangement of dislocations at the newly restructured boundaries, which are considered to be low angle grain boundaries. Restructuring, regardless of the mechanism, occurs at relatively low temperatures and is possibly contributed to by the presence of fission products in the fuel. Nucleation and growth are thought to start at fission product precipitates or bubbles and are expected to result in randomly oriented (high-angle) grains [7]. For polygonization, it is expected that the dislocation networks that ultimately cause grain subdivision are caused from fission gas bubbles or simply from irradiation damage [27]. These would result in low angle grain

boundaries. From this hypothesis, it is clear that fission gas bubbles, fission products, and microstructure all need to be thoroughly analyzed to better understand these mechanisms and fuel fragmentation. While this will be touched upon in detail in a future report, it is important to note here, as these grain boundary formations link directly with observed porosity (primarily created by fission gas bubbles) which are discussed in more detail in this report.

In this report, initial results from scanning electron microscopy (SEM), scanning transmission electron microscopy (S/TEM), and complimentary analytical tools will be discussed. Four samples are under consideration, with three having completed initial analysis and a fourth underway. Images collected using SEM were analyzed for average pore size as a function of radial position along the fuel rods. Energy dispersive x-ray spectroscopy (EDS) and electron backscatter diffraction (EBSD) data were also collected. In this work, preliminary EBSD data will be presented with the pore analysis as a function of sample burnup.

## 2. SAMPLE PREPARATION

Multiple samples have been selected for this work. Samples came from the North Anna powerplant. Here, we examine pre- and post- LOCA samples from fuel rods designated North Anna 1 and North Anna 2. The North Anna 1 rod experienced an average burnup of 63 GWd/tU, while the North Anna 2 rod experienced an average burnup of 68.5 GWd/tU. A cross section of these selected pellets was produced along the radial direction. Cross sections were polished and imaged using optical microscopy. An example micrograph of each of these samples is shown in Figure 2. There is a clear change between LOCA testing of the samples, particularly around the rim region where significant fragmentation is observed. These cross sections shown in the figure were further sectioned into pieces that included the cladding and extending into the fuel to near the center of the pellet. These regions were polished remotely in a hot cell in the Irradiated Fuels Examination Laboratory at Oak Ridge National Laboratory using a Buehler Minimet 1000 system. Once samples were polished, they were examined using a focused ion beam (FIB)/scanning electron microscope (SEM), specifically a ThermoFisher Scios2 DualBeam FIB/SEM adjacent to the hot cells and capable of examining radioactive specimen. The FIB/SEM was equipped with analytical tools including EDS and EBSD systems, both by EDAX. Pore size distributions were collected along the radial cross section using 2500× and 5000× magnification and a 20kV/0.8nA electron beam. EBSD data was collected at a 70° collection angle using a 20kV/6.4nA electron beam. Samples at selected regions across the fuel cross section were prepared for scanning/transmission electron microscopy (S/TEM) and complimentary EDS using the FIB/SEM, and preliminary results will be presented here.

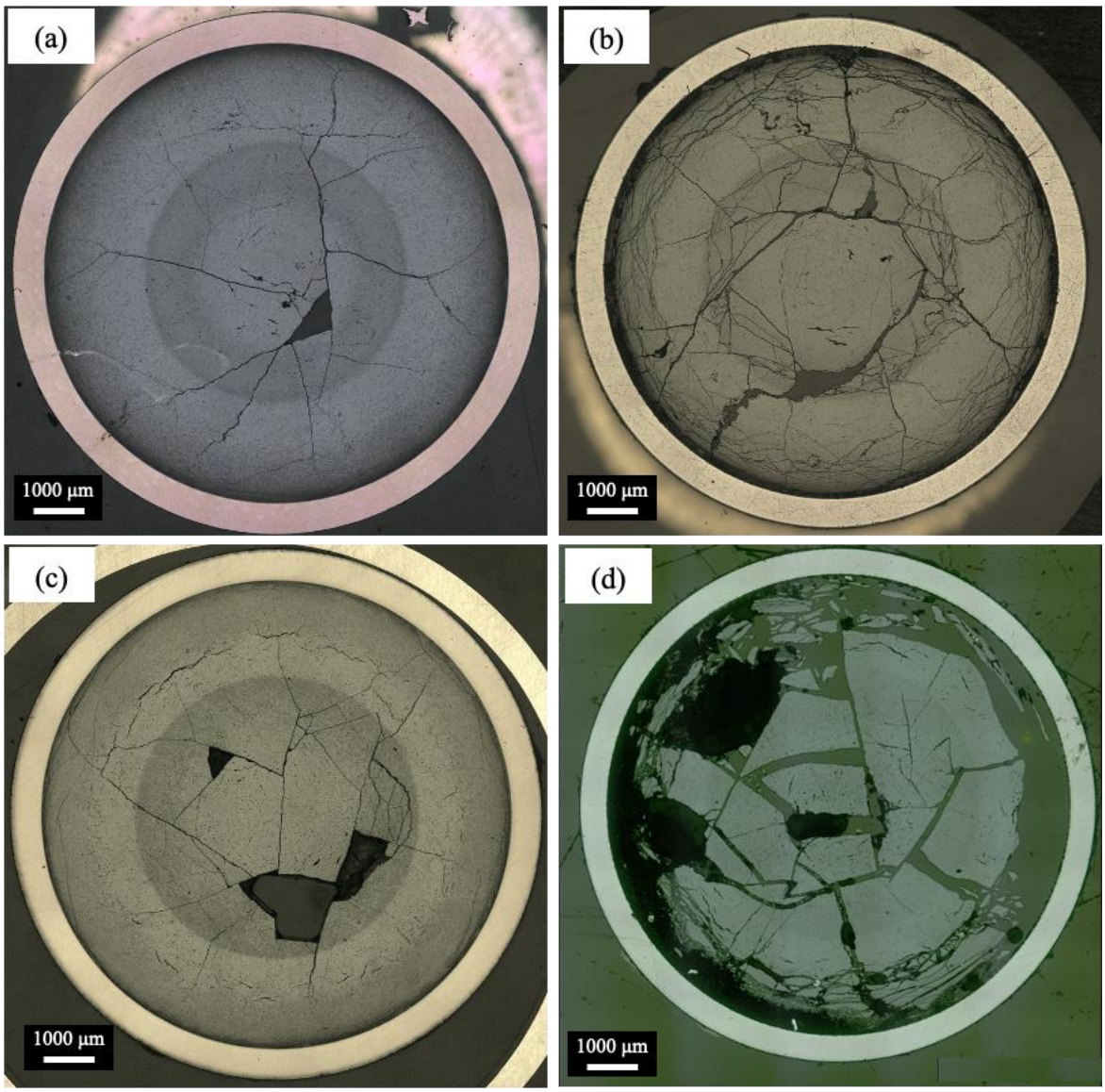


Figure 2: Optical micrographs of the four samples under examination: (a) the pre-LOCA North Anna 1 sample; (b) the post-LOCA North Anna 1 sample; (c) the pre-LOCA North Anna 2 sample; and (d) the post-LOCA North Anna 2 sample.

# 3. INITIAL MICROSTRUCTURE OBSERVATIONS

## 3.1 Pore Analysis

SEM images were collected, and the pore size distribution was analyzed and will be studied as a function of radius, local burnup, and LOCA testing (i.e., pre- vs. post-LOCA). A series of images were taken across the radius of the fuel at 2500× and 5000×. Images were analyzed using an ImageJ script to extract the average pore size and distribution. The script was calibrated by comparing to manual segmentation of the pores. The script's purpose is to measure the distance of each pore relative to the cladding/fuel interface. Before running the script, a circle is overlayed onto the image and measured to approximate the sample cross-section. The script functions by identifying all pores and finds the shortest distance from the pore to a point on the

fit circle. The output provides the pore size (in $\mu m^2$) and the distance to the cladding/fuel interface for each individual pore.

Data from this script was binned into 50 µm regions to assess the average pore size and total pore count. Binning is used for better visualization and to reduce noise in the data. The results of this analysis are shown in Figure 3. All data is plotted as a function of $r/r_0$, which defines the position along the radius of the fuel. The radial position is (r), and the radius of the fuel pellet is ($r_0$). This means that at the fuel-cladding interface, $r/r_0$ is approximately 1, and at the center of the fuel pin, $r/r_0$ is approximately 0. For the four samples, they had the following radius measurements: North Anna 1 pre-LOCA has $r_0$ = 4.21 mm; North Anna 1 post-LOCA has $r_0$ = 4.30 mm; North Anna 2 pre-LOCA has $r_0$ = 4.30 mm; and North Anna 2 post-LOCA has $r_0$ = 4.55 mm.

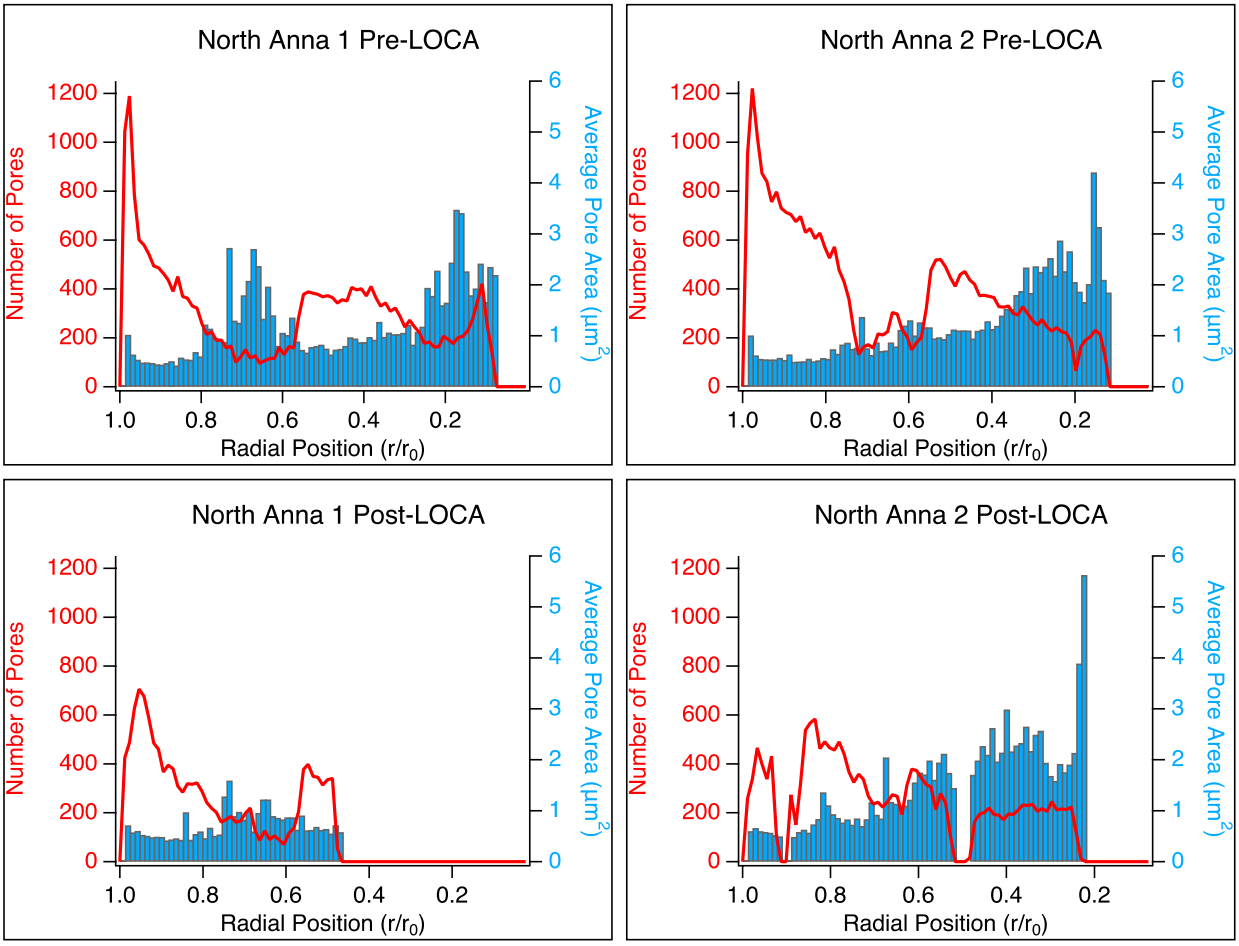


Figure 3: Pore count (number) and average pore area ($\mu m^2$) as a function of radial position in each fuel sample.

The pore analysis in the post-LOCA North Anna 1 sample stopped short just at the edge of the fuel/cladding interface due to extensive fuel fragmentation in the rim region that prevented data from being collected. Additionally, a portion of the final fuel cross section was not usable due to cracking during the preparation stages. Fragmentation also contributed to gaps in the post-LOCA North Anna 2 sample. There is a trend of a decreasing number of pores near the fuel/cladding

interface as a function of LOCA testing. Otherwise, the samples follow the general trend of having a high pore density (but lower average pore area) at $r/r_0 \sim 1$, and again at around $r/r_0 \sim 0.5$. At $r/r_0 \sim 0.75$, there is an increase in average pore area, but a decrease in the total pore numbers in that region. This same phenomenon happens again closest to the center of the fuel, at $r/r_0 \sim < 0.3$. Observed pores generally increase in size but the number of pores (pore count) decreases with further distance from the fuel/cladding interface (i.e., moving closer to the pellet centerline). In the region adjacent to the cladding, the pores are small, highly circular, and dense. Moving radially inward, there is a noticeable difference in pore structure in the mid-radial region of the fuel pellet. The number of pores is noticeably lower and the shape of the pores diverge from spherical shapes with a larger degree of oblateness. Near the pellet centerline, the pores begin increasing in size and decrease in ovality to a more circular shape. These observations support the presence of distinct microstructural regions (rim, transition, and center) across the fuel pin, and can be observed in Figure 4, Figure 5, Figure 6, and Figure 7. Additionally, an example of the pore size and shape as a function of radial position is shown in Table 1. This example in Table 1 shows the average pore size at a specified location in the North Anna 1 Pre-LOCA sample, and the average circularity, defined as $4\pi\left(\frac{Area}{Perimeter^2}\right)$. In this initial examination, all pores less than 0.05μm in diameter were not considered for part of the analysis due to difficulty differentiating them at the chosen scale at 2500×.

Table 1: Example pore properties from the North Anna 1 Pre-LOCA fuel sample

| Approximate $r/r_0$ | Average Pore Diameter (μm) | Average Pore Circularity |
|---|---|---|
| 1.0 | 1.03 | 0.77 |
| 0.95 | 0.92 | 0.79 |
| 0.90 | 0.95 | 0.77 |
| 0.85 | 1.06 | 0.75 |
| 0.75 | 1.39 | 0.67 |
| 0.65 | 1.49 | 0.64 |
| 0.50 | 1.18 | 0.66 |
| 0.30 | 1.51 | 0.69 |

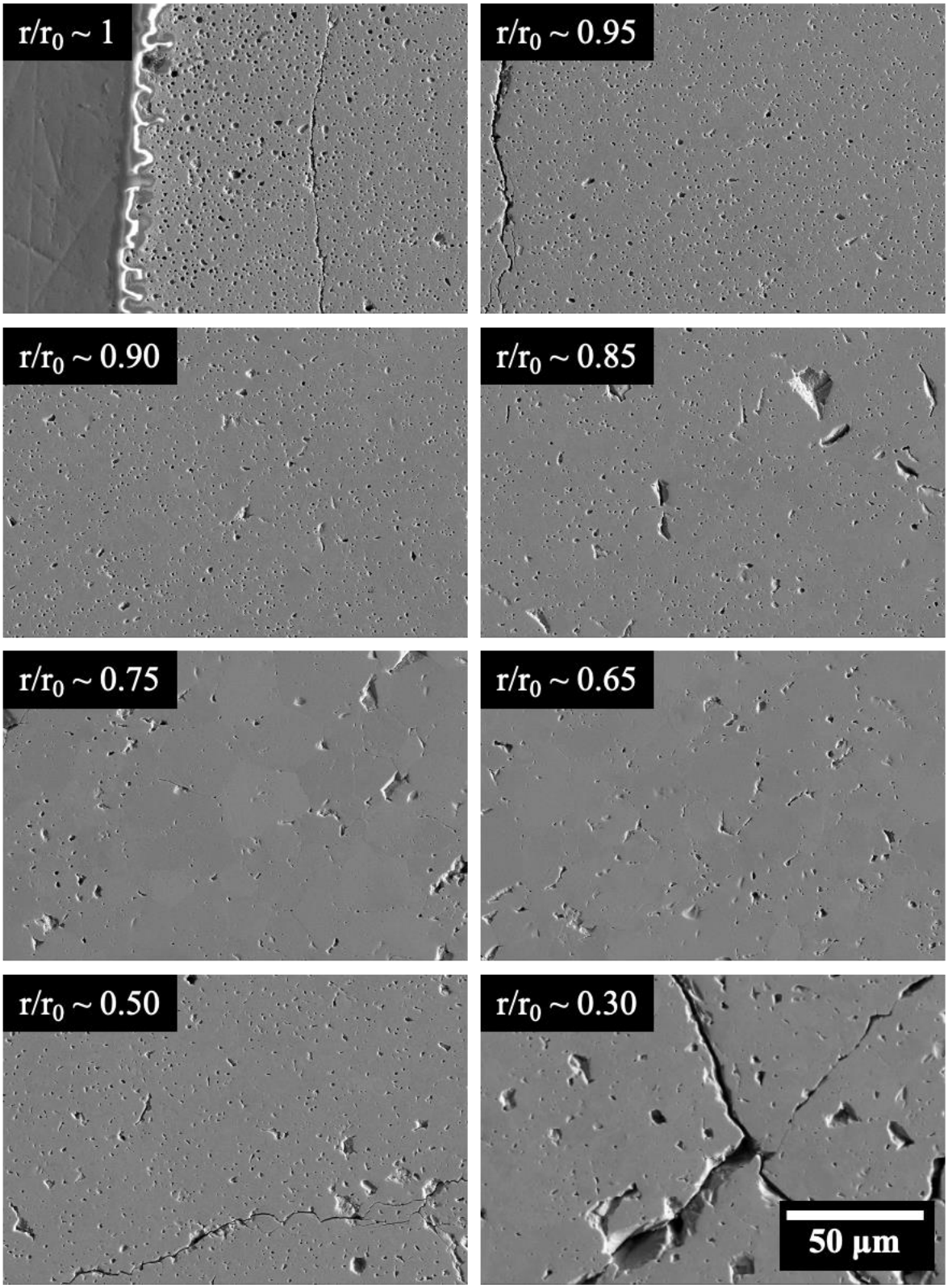


Figure 4: SEM micrographs along the North Anna 1 Pre-LOCA fuel cross section at various radial positions, which highlight the variation in microstructure and pore structure.

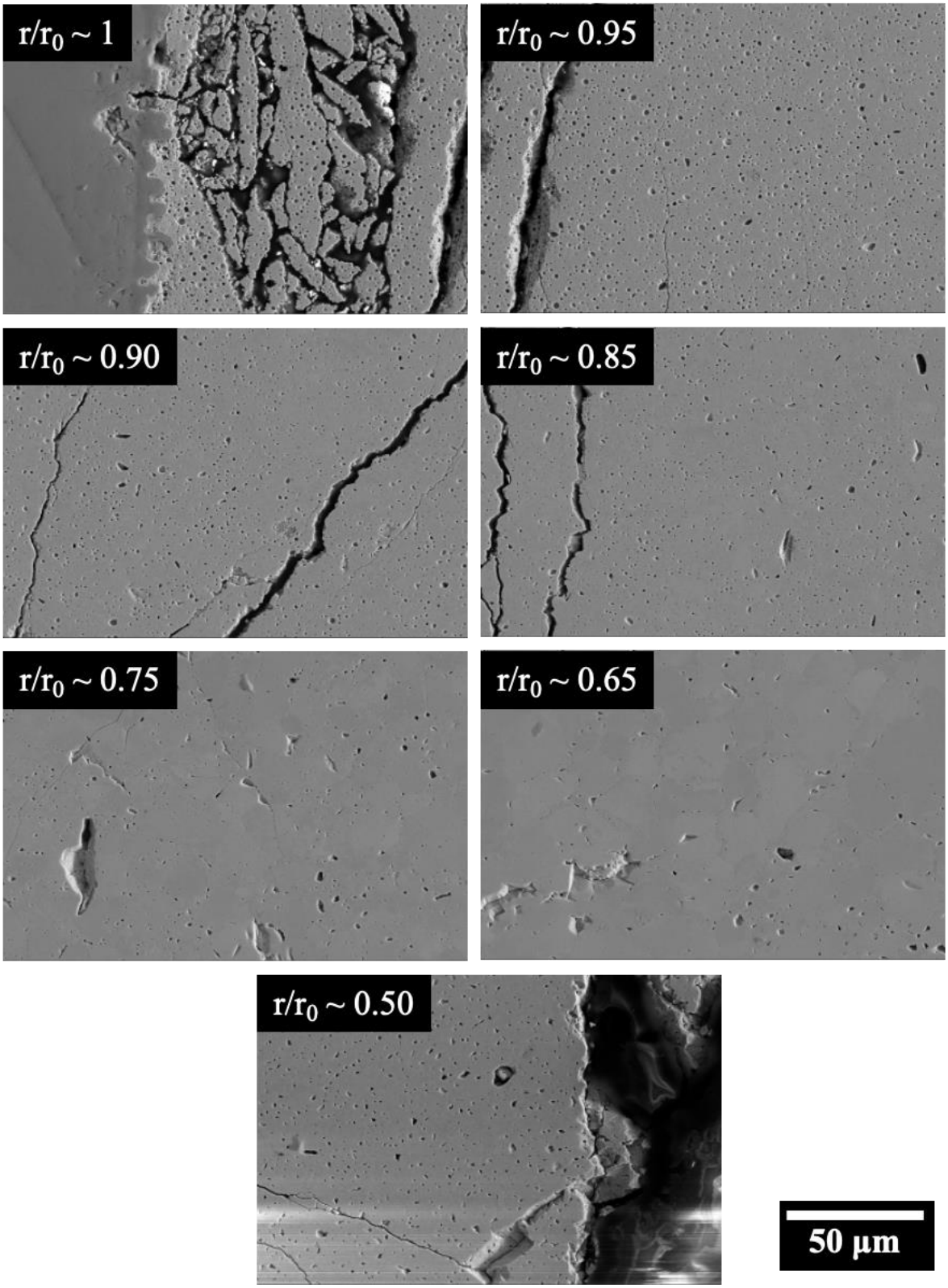


Figure 5: SEM micrographs along the North Anna 1 Post-LOCA fuel cross section at various radial positions, which highlight the variation in microstructure and pore structure.

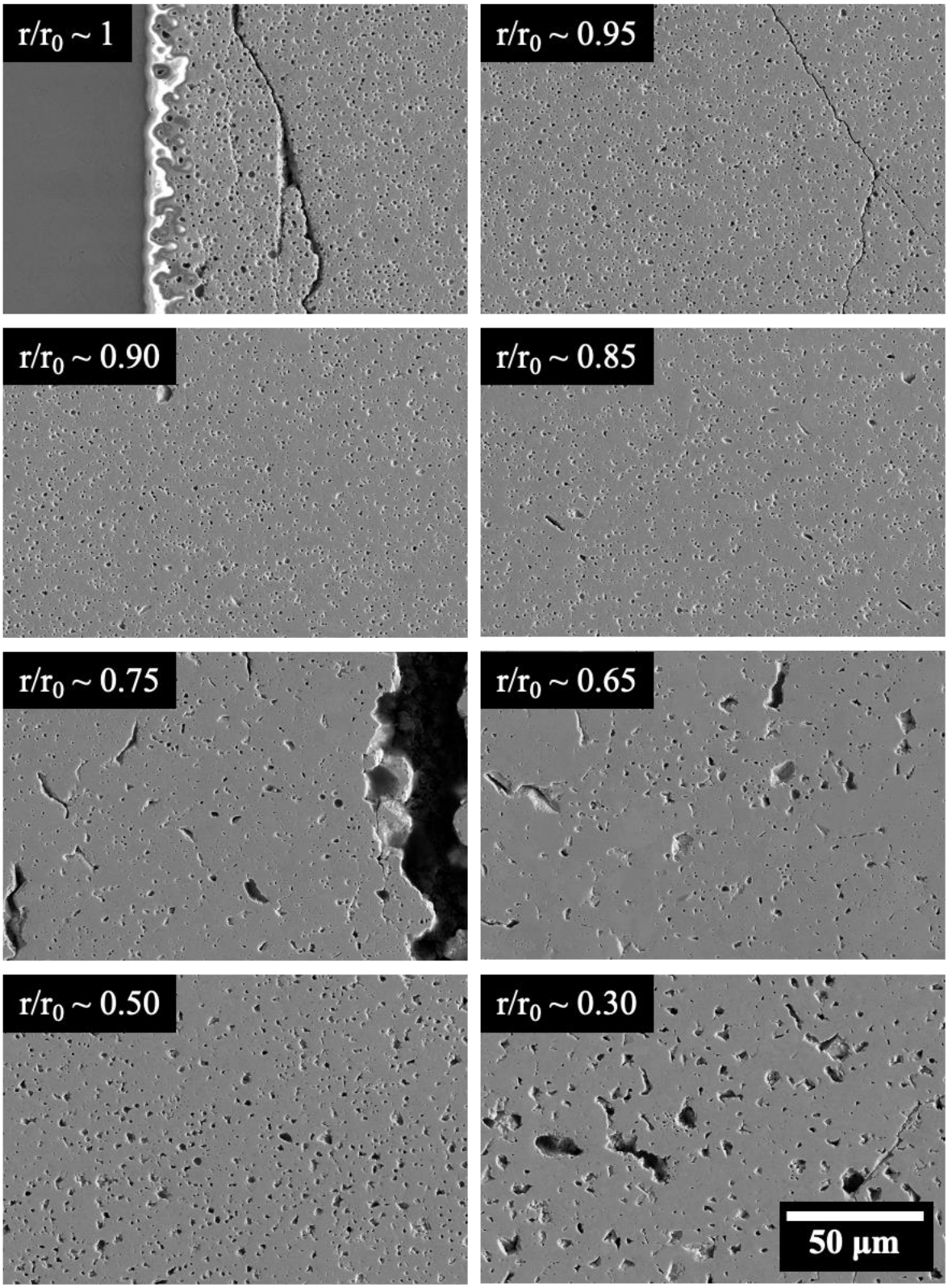


Figure 6: SEM micrographs along the North Anna 2 Pre-LOCA fuel cross section at various radial positions, which highlight the variation in microstructure and pore structure.

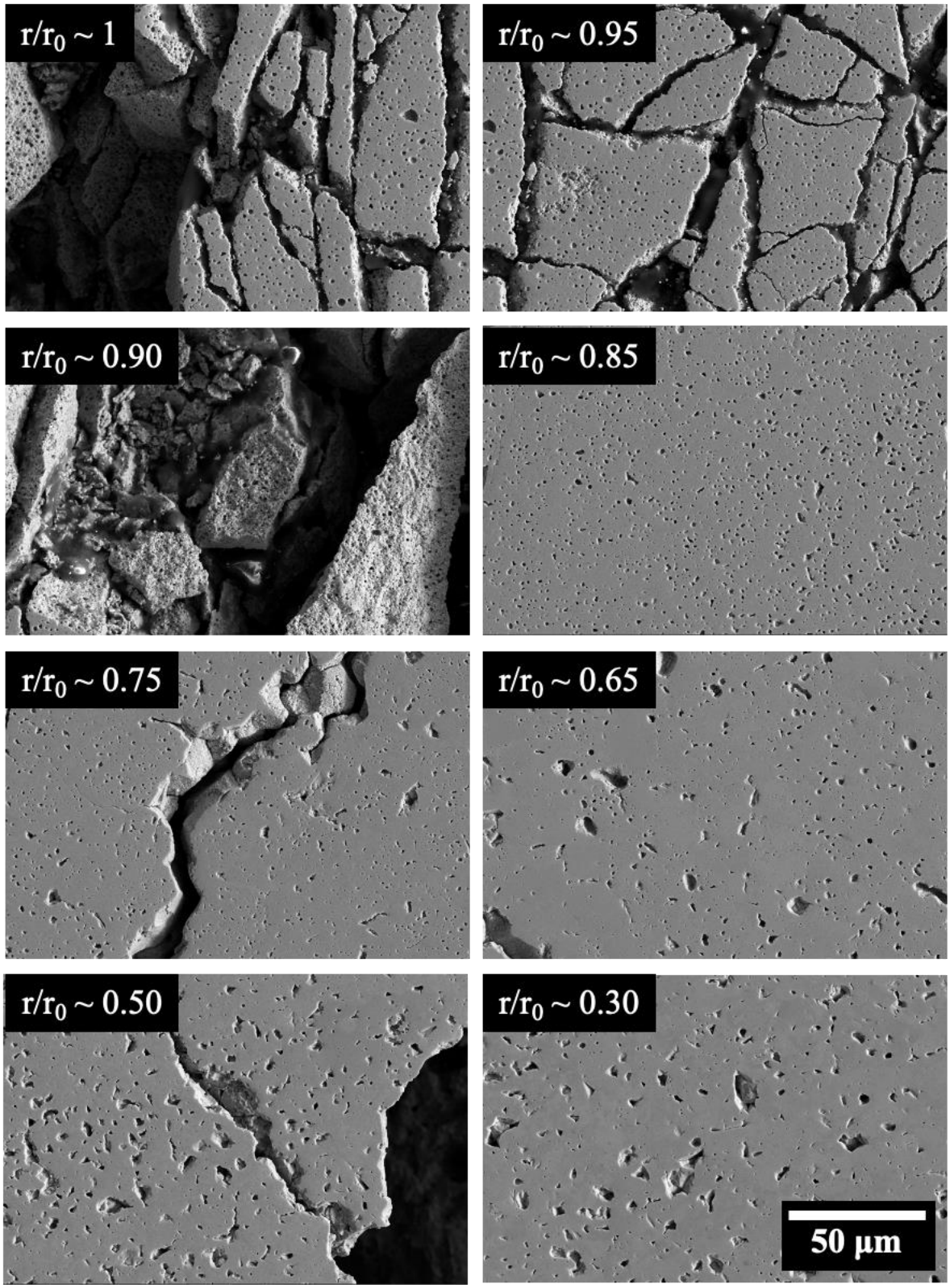


Figure 7: SEM micrographs along the North Anna 2 Post-LOCA fuel cross section at various radial positions, which highlight the variation in microstructure and pore structure.

## 3.2 Grain Structure

EBSD data was collected to determine average grain size and grain misorientation trends in relation to fracture, pores, and a function of burnup (i.e., radial location). An example dataset from the North Anna 1 Pre-LOCA sample is shown in Figure 8. The smallest grains are found on the pellet periphery, which complements findings from Gerczak et. al. [25]. Grain boundaries are classified by the misorientation of the adjacent grains, where low angle grain boundaries (LAGBs) are considered to have < 15° misorientation and high angle grain boundaries (HAGBs) have > 15° misorientation. These are considered to be distinct classes based on differences in the local structure necessary to accommodate the grain boundary [28]. As discussed in detail in [25], LAGBs are made up of dislocation cores and caused by sub-division of larger grains. Within approximately 500 microns of the pellet/cladding interface and at the fuel center, HAGBs dominate the microstructure. However, mid-radially, HABGs decrease below half the grain boundary fraction. These observations suggest new grain boundaries are being formed in the transition regions of the high burnup fuel, and like in the work of [25], implies LAGBs may evolve into HAGBs during irradiation. In the fuel center, there is another increase in HAGB character fraction. When compared back to Figure 3, while initially it would appear that high HAGB fraction near the fuel/cladding interface correlates with the high number of pores, the trend does not continue further into the material. Instead, inside the fuel there does not appear to be any discernable correlation directly between pore size and number density as a function of HAGB character fraction. However, a detailed grain boundary characterization and grain size evaluation of all samples is still underway.

EDS data was also collected to study the distribution of elements across the fuel pellet. From the low magnification overview, there was no significant variation in elemental distribution across the fuel pin. However, most observed fission products like Xe may be too small to detect on this level at the count rate used, leaving the results to need refining.

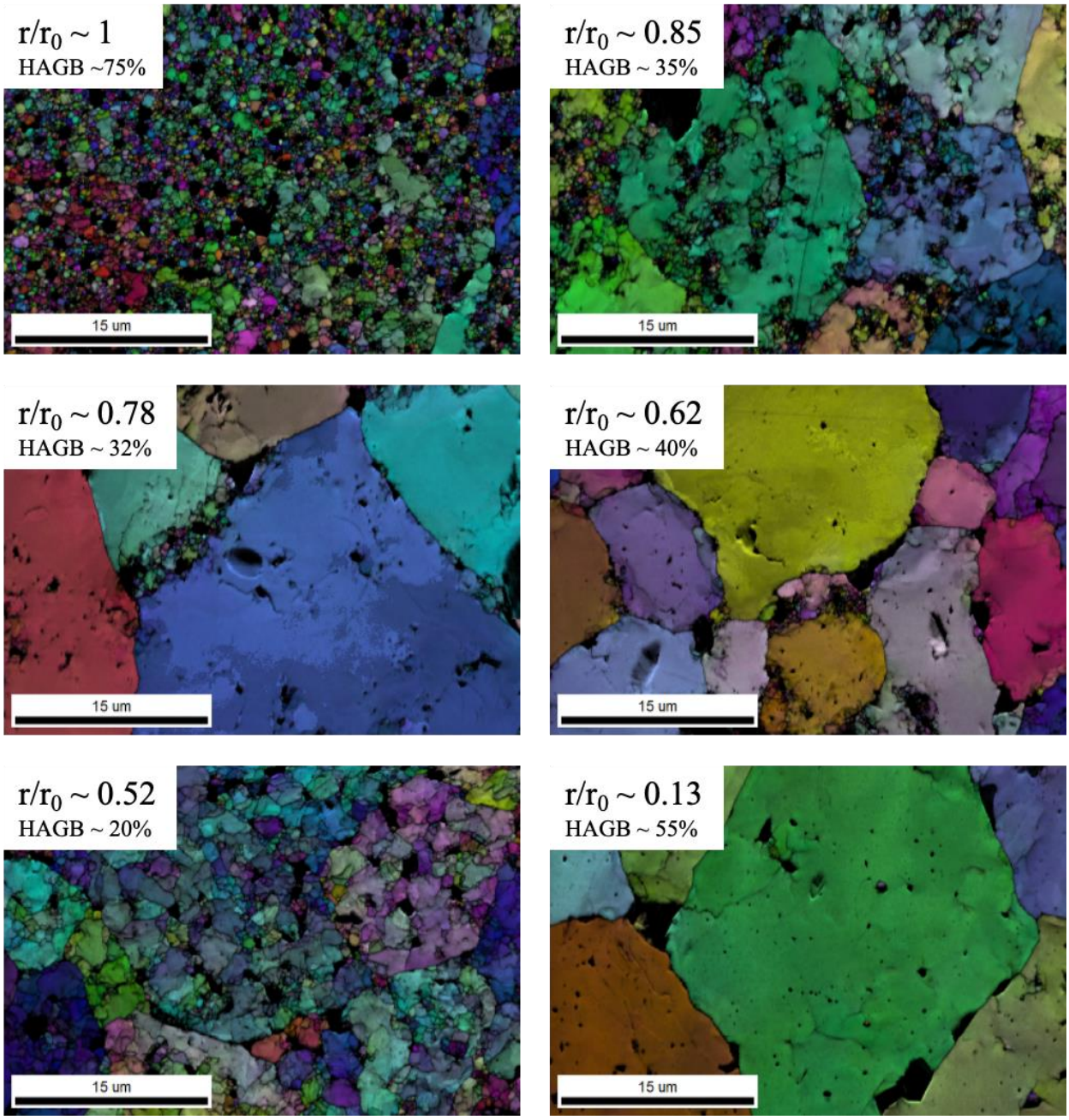


Figure 8: An example of the observed grain structure as a function of distance to pellet/cladding interface. This example is from the North Anna 1 Pre-LOCA sample. The HAGB character fraction (in a percentage) is indicated for each region underneath the radial position.

## 3.3 Preliminary STEM Analysis

Specific radial locations along the fuel pin were targeted for STEM/EDS analysis to compliment EBSD and SEM results. STEM/EDS aims to target microstructure and chemical information on the nanometer length scale. Lamella were taken at various distances from the fuel/cladding interface. Lamella were prepared using a ThermoFisher Scios2 FIB/SEM Dualbeam and were created under standard procedures. A 200kV ThermoFisher Talos F200X S/TEM was used to collect all data, equipped with a SuperX 4-detector EDS system [29]. Elemental mapping was

completed using ThermoFisher MAPS automation software to allow large areas to be mapped without human supervision; an example is shown in Figure 9. The analysis showed nanometer-scale Xe gas bubbles located both intragranuarly and along grain boundaries, and in company of five-metal particles. Results are still pending to see if Xe gas features were observed in the restructured transition areas of the fuel, as they were not observed in these regions in a previous work [25]. This data is preliminary, and transmission Kikuchi diffraction may also be completed on targeted liftouts to further study the microstructure of the fuel on a higher order of magnitude spatial resolution.

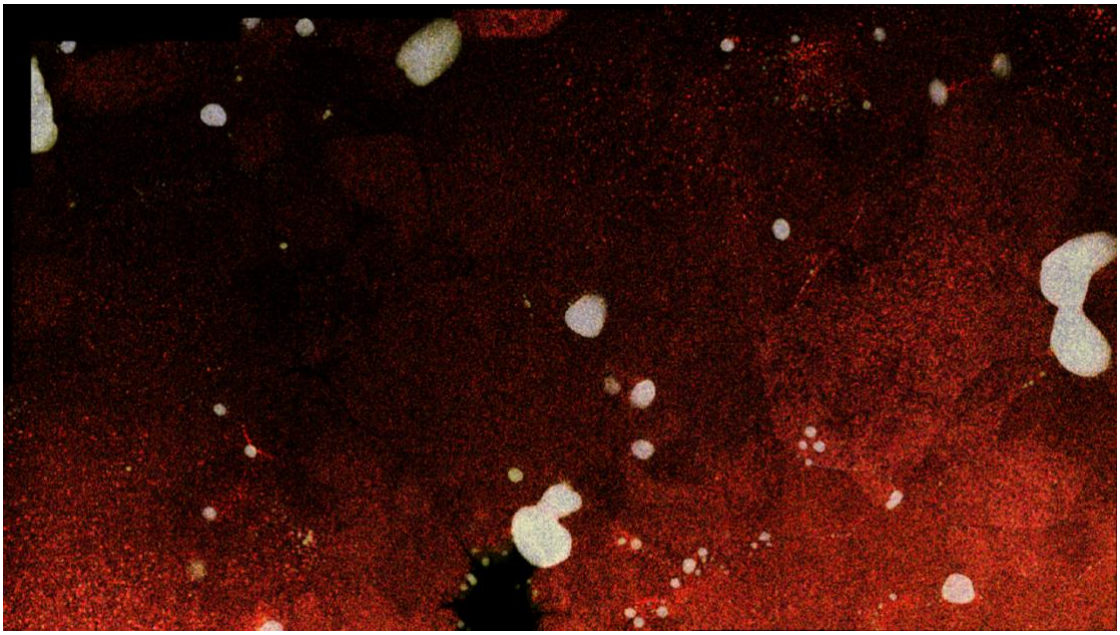

Figure 9: STEM/EDS map indicating Xe bubbles (red) along grain boundaries and intragranularly in a liftout from 100 µm distance from the fuel/cladding interface. Red: Xe. Yellow: Mo+Tc+Ru. Blue: Rh+Pd. White: blue+yellow (i.e., five metal particles).

# 4. CONCLUSIONS

This report presents initial microstructural observations of fuel samples from high burnup commercial fuel rods with varying operational histories. This work is preliminary, and therefore extensive conclusions have not yet been drawn from the results. Data indicates a clear correlation between pore size and shape with radial location across the fuel pin. However, only some correlations between HAGB character and pore density and shape can be seen, especially at the fuel/cladding interface. Additionally, Xe density appears to also be related to this radial positioning. EBSD data indicates that smaller grains are found on the pellet periphery, and that grain boundary information suggest new grain boundaries are being formed in the transition regions of the high burnup fuel. This implies that LAGBs may form HAGBs during irradiation. Detailed grain boundary, elemental, and microstructural characterization are underway and will culminate in a more thorough reported and a peer-reviewed publication.

# 5. ACKNOWLEDGEMENTS

This work was supported by the Advanced Fuels Campaign within the Department of Energy, Office of Nuclear Energy. The authors would like to acknowledge Tyson Jordon and the 3525 hot cell operators in the Irradiated Fuels Examination Laboratory for their assistance with sample handling and preparation.

# 6. REFERENCES

1. J. Noirot et al., "Size and Radial Origin of Fragments formed while heating a 83 GWd/tU PWR Fuel up to 1200ºC", Minutes of the HRP-WGFS workshop on fuel fragmentation, relocation and dispersal, Aix en Provence May 2015, by Wolfgang Wiesenack. HWR-1147, July 2015
2. M. Bruet, *et al.*, "High burn-up fuel behaviour during a LOCA type accident: the FLASH 5 experiment", IAEA Technical Committee Meeting on Behavior of Core Materials and Fission Product Release in Accident Conditions in LWR's, 1992, Cadarache, France.
3. Y. Yang, Z.M. Burns,T.S. Smith, K.D. Linton, K. Yueh, and K.A. Terrani, LOCA Fragmentation Test with High Burnup HBR Fuel Rod. United States: N. p., 2020
4. K. Une, S. Kashibe & A. Tagaki, "Fission Gas Release Behavior from High Burnup $UO_2$ Fuels under Rapid Heating Conditions", Journal of Nuclear Science and Technology, 43:9, p. 1161-1171 (2006). DOI: 10.1080/18811248.2006.9711208
5. K. Une, S. Kashibe & K. Hayashi, "Fission Gas Release Behavior in High Burnup $UO_2$ Fuels with Developed Rim Structure", Journal of Nuclear Science and Technology, 39, p. 668-674 (2002). DOI: 10.1080/00223131.2002.10875557
6. E. Thomas, C.E. Beyer, L.A. Charlot, "Microstructural analysis of LWR spent fuels at high burnup," Journal of Nuclear Materials, 188, p. 80-89 (1992).
7. K. Nogita, K. Une, "'Irradiation induced recrystallization in high burnup UO2 fuel," Journal of Nuclear Materials, 226, p. 302-310 (1995).
8. M. E Cunningham, M. D. Freshley, D. D. Lanning, "Development and characteristics of the rim region in high burnup UO2 pellets," Journal of Nuclear Mateirals, 188, p.19-27 (1992)
9. K. Une, K. Nogita, S. Kashibe, T. Toyonaga, M. Amaya, *Proc. of the Int. Topical Mtg. on LWR Fuel Performance*, Portland, p.478 (1997).
10. C.T. Walker, "Assessment of the radial extent and completion of recrystallisation in high burn-up $UO_2$ nuclear fuel by EPMA," Journal of Nuclear Materials, 275, 56-62 (1999).
11. M. Mogensen, J.H. Pearce, C.T. Walker, "Behaviour of fission gas in the rim region of high burn-up $UO_2$ fuel pellets with particular reference to results from an XRF investigation," Journal of Nuclear Materials, *264*, 99-112 (1999).
12. K. Une, M. Hirai, K. Nogita, T. Hosokawa, Y. Suzawa, S. Shimizu, Y. Etoh, "Rim structure formation and high burnup fuel behavior of large-grained $UO_2$ fuels," Journal of Nuclear Materials,278, 54-63 (2000).
13. W. Wiesenack, "Summary of the Halden Project LOCA Test Series IFA-650", HPR-380, OECD NEA Halden Reactor Project, May 2013
14. L. Lekkonen, "LOCA Testing in Halden, the Fourth Experiment: IFA-650.4", HWR-838, OECD Halden Reactor Project, January 2007

15. B.C. Oberlander, M. Espeland and N. O Solum, “PIE results from the high burnup (92 GWd/MTU) PWR segment after LOCA testing in IFA 650-4”, Proc. Of the EHPG meeting, Sandefjord 2011
16. P. A. C. Raynaud, “Fuel Fragmentation, Relocation, and Dispersal during Loss-of-Coolant Accidents”, US NRC, Office of Nuclear Regulatory and Research, NUREG-2121, March 2012
17. M Flanagan, P. Askeljung, A. Purana, “Post-Test Examination Results from Integral High Burnup Fuelded LOCA Test at Studsvik Nuclear Laboratory”, US NRC, Office of Nuclear Regulatory and Research, NUREG-2160, August 2013
18. P. Askeljung, J. Flygare, and D. Minghetti, ‘‘NRC LOCA Testing Program at Studsvik, Recent Results on High Burnup Fuel,’’ Proc. 2012 Top Fuel Conf., Manchester, United Kingdom, September 2–6, 2012.
19. K. Une, S. Kashibe, and A. Takagi, “Fission Gas Release Behavior from High Burnup $UO_2$ Fuel at Rapid Heating Conditions”, Proc. 2005 Water Reactor Fuel Performance Meeting Oct 3-6 2005
20. “Report on Fuel Fragmentation, Relocation, Dispersal,” Nuclear Energy Agency, Committee on the Safety of Nuclear Installations,” NEA/CSNI/R(2016)16,October 2016
21. E. Kolstad et. al., “High Burnup Fuel Behavior under LOCA Conditions as observed in Halden Experiments”, Fuel Behavior and Modelling under Severe Transient and Loss of Coolant Accident (LOCA) Conditions. Proceedings of a Technical Meeting, Mito, Japan, 18-21 October 2011. IAEA-TECDOC-CD-1709
22. Y. Pontillon et al., “Experimental and theoretical investigation of fission gas release from $UO_2$ up to 70 GWd/tU under simulated LOCA type conditions”, paper 1025, Proc 2004 Int. Meeting on LWER Fuel Performance, Orlando, Florida, September 19–22 (2004).
23. M. Marcet et al., “Contribution of high burnup structure to fission gas release under transient conditions”, paper 2005, Proc. Top Fuel, Paris, France, 6–10 September (2009).
24. M. Marcet, “Etude de la fracturation mecanique de la structure a haut de combustion des combustible irradies (RIM) en traitment thermeque”, Universite d’Aix-Marseille December 2010RIL 2021-13 “Interpretation of Research on Fuel Fragmentation, Relocation, and Dispersal at High Burnup”, December 2021
25. Gerczak, T.J., C.M. Parish, P.D. Edmondson, C.A. Baldwin, K.A. Terrani, “Restructuring in high burnup UO2 studied using modern electron microscopy,” Journal of Nuclear Materials 509, p. 245-259 (2018)
26. V. V Rondinella, T. Wiss, “The high burn-up structure in nuclear fuel, Materials” Today, 13 p. 24–32 (2010).
27. H. Matzke, J. Spino, “Formation of the rim structure in high burnup fuel,” Journal of Nuclear Mateirals 248, p.170-179, (1997).
28. A.P. Sutton, R.W. Balluffi, H. Lüth, J.M. Gibson, “Interfaces in Crystalline Materials and Surfaces and Interfaces of Solid Materials”, Physics Today 49, p.88 (1996).

29. C.M. Parish, MT3FT-15OR0204122: Report on the acquisition and installation of FEI Talos F200X S/TEM, Oak Ridge National Laboratory, Oak Ridge, TN (United States), 2015.